THE JOURNAL OF PHYSICAL CHEMISTRY A
A JOURNAL OF THE AMERICAN CHEMICAL SOCIETY

Open Access
This article is licensed under CC-BY-NC-ND 4.0

pubs.acs.org/JPCA
Article

Gas-Phase Benzene−Methanol Dimer Configurations: Geometries, Relative Stabilities, and Interaction Energies

Karl N. Kirschner*

Cite This: J. Phys. Chem. A 2025, 129, 8110−8119
Read Online

ACCESS | Metrics & More | Article Recommendations | Supporting Information

ABSTRACT: The benzene···methanol dimer is one of the simplest systems that manifests an O−H···π nonbonded interaction. This interaction can be found in numerous systems, ranging from small-molecule clusters to biological systems, for example, phenyl-containing ligands bound within a protein's binding pocket. Herein, four gas-phase configurations are examined using quantum mechanics, which have O−H···π, CH_3···π and Bz−H···O interactions. Geometry optimization and frequency calculations were performed up to the MP2/aug-cc-pVQZ theory level, with electronic energies obtained up to the CCSD(T)/complete basis set (CBS) limit. Considering the electronic energy (ΔE_{el}), the O−H···π configuration is the most stable, with a CCSD(T)/CBS (counterpoise corrected) interaction energy of −4.09 kcal mol^{-1}, while the other three configurations ranged from −2.00 to −2.60 kcal mol^{-1}. Using scaled harmonic frequencies, the temperature influence was investigated by computing Gibbs relative and interaction free energies over a 10−800 K temperature range.

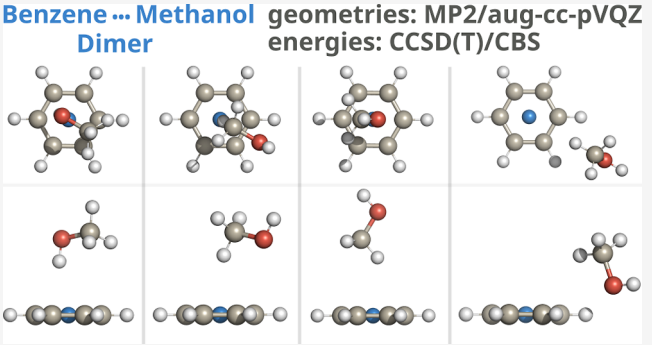

INTRODUCTION

The nonbonded interactions of π-containing molecules have long been of interest in chemistry.[1] The benzene (BZ) and methanol (MeOH) nonbonded dimer fundamentally represents the interaction between a molecule with delocalized π electrons and an organic molecule capable of hydrogen bonding. The intermolecular forces that enable this dimer's formation are prevalent in biopolymer systems, assisting in stabilizing conformations and the binding of ligands. Several nonbonded configurations are conceptually possible: the hydroxyl group interacting with the π molecular orbital above the ring (i.e., O−H···π), the methyl group interacting with the π orbital (i.e., CH_3···π), and BZ's hydrogen interacting with the oxygen atom (i.e., Bz−H···O). Each configuration has subtle spatial orientations that depend on how MeOH orients itself. For example, does the methyl group lie bisected between two BZ-H bonds or directly over one BZ−H bond?

Recently, Di Mino et al. reported the experimental observation of how BZ and MeOH interact in a 1:19 ratio solution by using neutron diffraction combined with hydrogen isotopic substitution.[2] Their data shows the O−H···π configuration, with an additional MeOH interaction around BZ's plane. Based on these results, they elegantly formulated the idea that the BZ···MeOH interactions can be categorized as either out-of-plane (e.g., O−H···π) or in-plane (i.e., Bz−H···O).

Concerning gas-phase quantum mechanics investigations that isolate BZ···MeOH in a 1:1 ratio, a limited number of studies have been done, as summarized in Table 1. Matisz et al. investigated the most configurations, three, with MP2 and DFT optimizations performed using the 6-31+G(d,p) basis set.[3] Regarding the interaction energies, a CCSD(T)/complete basis set (CBS) value for the O−H···π configuration was computed by Řezáč et al.—whose geometry was optimized at MP2/cc-pVTZ, with the nonbonded distance minimum interpolated from the CCSD(T)/CBS dissociation curve.[4,5] These data are part of the S66 database. For two configurations, Marchione and McCoustra performed the most rigorous calculations, with an approximated CCSD(T)/aug-cc-pVTZ//MP2/aug-cc-pVDZ theory level.[6] Frequency calculations have been limited to two configurations, with the 6-31+G(d), 6-31G(d,p) and 6-31+G(d) basis set used.[6−9]

While previous investigations covered three configurations with electron-correlated and DFT approaches using a variety of basis sets, there lacks a more definitive study that firmly establishes the configurations' relative stabilities, electronic interaction energies, and harmonic vibrational frequencies. Furthermore, there has been no exploration of how the Gibbs free energies might vary with the temperature. Herein, we report the optimized geometries and scaled frequencies computed using the MP2/aug-cc-pVQZ theory level for four configuration

Received: June 6, 2025
Revised: July 30, 2025
Accepted: July 31, 2025
Published: August 23, 2025

ACS Publications
© 2025 The Author. Published by American Chemical Society

https://doi.org/10.1021/acs.jpca.5c03923
J. Phys. Chem. A 2025, 129, 8110−8119

Table 1. Previous Theoretical Calculations Performed on the BZ···MeOH Dimer

theory	configurations	references
Full Optimizations		
MP2/6-31+G(d)//MP2/6-31+G(d)	1	9
MP2/6-31+G(d,p)//MP2/6-31+G(d,p)	3	3
B3LYP/6-31+G(d)//B3LYP/6-31+G(d)	1	7−9
BP86/TZVP//BP86/TZVP	1	10
BP86-D/TZVP//BP86-D/TZVP[a]	1	10
PBE-D/TZVP//PBE-D/TZVP[a]	1	10
MPWB1K/6-31+G(d,p)//MPWB1K/6-31+G(d,p)	3	3
M06-2X/6-31+G(d,p)//M06-2X/6-31+G(d,p)	3	3
MP2/aug-cc-pVDZ//MP2/aug-cc-pVDZ	2	6
MP2/cc-pVTZ//MP2/cc-pVTZ	1	4 and 5
Interaction Energies		
M06-2X/6-311++G(d,p)//MP2/6-31+G(d,p)	3	3
MP2/6-311++G(d,p)//MP2/6-31+G(d,p)	3	3
MP2/aug-cc-pVDZ//MP2/6-31+G(d,p)	3	3
MP2/aug-cc-pVTZ//MP2/6-31+G(d,p)	3	3
MP2/aug-cc-pVQZ//MP2/6-31+G(d,p)	3	3
MP2/CBS//MP2/6-31+G(d,p)[b]	3	3
MP2/aug-cc-pVTZ//MP2/aug-cc-pVDZ	2	6
CCSD(T)/aug-cc-pVTZ//MP2/aug-cc-pVDZ[c]	2	6
CCSD(T)/CBS//MP2/cc-pVTZ	1	4 and 5
Frequencies		
MP2/6-31G(d,p)//MP2/aug-cc-pVDZ	2	6
MP2/6-31+G(d)//MP2/6-31+G(d)	1	9
B3LYP/6-31+G(d)//B3LYP/6-31+G(d)	1	7−9

[a]The -D indicates that an empirical dispersion correction term was added. [b]The CBS energy values were determined using MP2/aug-cc-pVnZ//MP2/6-31+G(d), where n = 2, 3, and 4. [c]The CCSD(T) energy was approximated as E(MP2/TZ) + ΔCCSD(T), where ΔCCSD(T) was computed from CCSD(T)/cc-pVDZ and MP2/cc-pVDZ.

minima, as well as the electronic and free interaction energies computed using CCSD(T)/CBS//MP2/aug-cc-pVQZ.

METHODOLOGY

Nonbonded interactions will be defined using a donor··· acceptor notation, where the donor and acceptor possess local positive and negative electrostatic environments ($\delta^+\cdots\delta^-$), respectively. Thus, the following notations will be used: O−H···π, CH_3···π, and Bz−H···O, where π indicates interaction with BZ's delocalized electrons.

All optimization and frequency calculations were performed using Psi4 (v. 1.7; Git Rev 6ce35a5). MP2 and CCSD(T) calculations, correlating valence electrons only, were performed using the aug-cc-pVDZ (aDZ), aug-cc-pVTZ (aTZ), and aug-cc-pVQZ (aQZ) basis sets.[11] Unless otherwise noted, theory levels indicate that the reported data were computed by using the optimized geometry determined at the same level (e.g., MP2/aQZ formally stands for MP2/aQZ//MP2/aQZ). All calculations involving the aTZ basis set were truncated to adjust the minimum eigenvalue overlap cutoff criteria to a tolerance of 1.0×10^{-6} (i.e., "s_tolerance"), except for the calculations that explored the effects of retaining the full molecular orbital set.

All optimizations were performed in Cartesian space, without geometric restraints, with convergence criteria of a maximum force of 1.5×10^{-5}, an RMS force of 1.0×10^{-5}, a maximum displacement of 6.0×10^{-5}, and an RMS displacement of 4.0×10^{-5} hartree atomic unit^{-1} (i.e.,"g_convergence gau_tight"). Vibrational frequencies were determined by using finite gradient differences. The CBS Hartree−Fock energies were estimated using Halkier's two and three consecutive basis set schemes, while the correlated energies were estimated using Halkier's two consecutive basis set scheme, always using the two largest basis sets listed in the stated labels.[12,13] To unambiguously indicate this, the nomenclature CBS(a[mno]Z) will be used, where m, n, and o represent the basis set cardinal numbers. All calculations were performed used density-fitted algorithms.[14−19]

To correct for harmonic approximations,[20] all vibrational frequencies were scaled. Optimized scaling factors for the MP2/aQZ frequencies were determined using SciPy's Brute-force algorithm,[21] specifying a search range between −10 and 10. The following loss function was defined that represents the mean average error between the scaled MP2/aQZ and target experimental frequencies:

$$\text{Loss} = \frac{\sum_n |(\sigma \times \nu_n^{\text{MP2/aQZ}}) - \nu_n^{\text{Exp.}}|}{n} \quad (1)$$

where σ is a scaling factor and ν_n represents the individual frequencies. The methanol and benzene monomer-computed vibrational modes were assigned through a visual inspection and comparison to their experimental characterization.[22,23] The experimental benzene values chosen followed the curation done by Miani et al.[24] The optimized scaling factors (ν <1000 cm^{-1}: 0.9911 and ν >1000 cm^{-1}: 0.9523) were subsequently applied to the dimer frequencies.

Interaction energies were computed based on the chemical equation $C_6H_6 + CH_3OH \rightleftarrows C_6H_6\cdots CH_3OH$ using the following three approaches:

$$\Delta E = E_{AB}^{\alpha\cup\beta}(AB) - E_A^{\alpha}(A) - E_B^{\beta}(B) \quad (2)$$

$$\Delta E_{CP} = E_{AB}^{\alpha\cup\beta}(AB) - E_{AB}^{\alpha\cup\beta}(A) - E_{AB}^{\alpha\cup\beta}(B) \quad (3)$$

https://doi.org/10.1021/acs.jpca.5c03923
J. Phys. Chem. A 2025, 129, 8110−8119

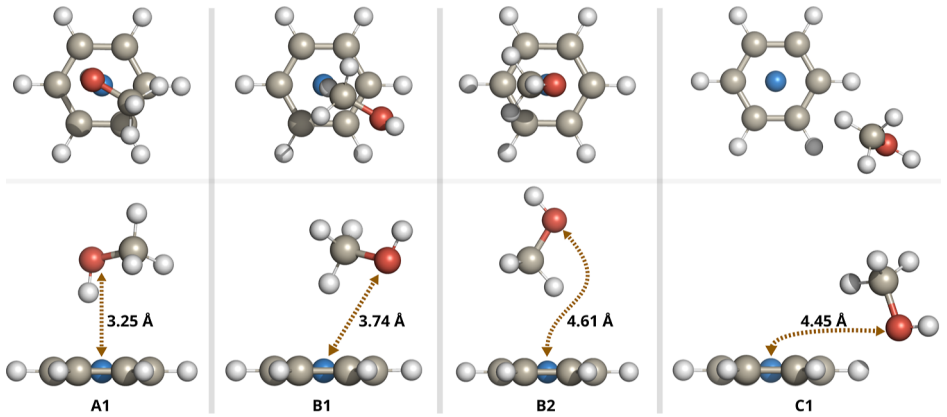

Figure 1. MP2/aQZ fully optimized nonbonded configurations of the BZ···MeOH dimer. The bottom structures are a −90° x-axis rotation of the top structures. The centroid defined by benzene's atoms is represented by a blue sphere for each configuration. The distances between methanol's oxygen and the benzene's centroid are labeled (see Table 2).

$$\Delta E_{Rig} = E_{AB}^{\alpha\cup\beta}(AB) - E_{AB}^{\alpha\cup\beta}(A) - E_{AB}^{\alpha\cup\beta}(B) + [E_{AB}^{\alpha}(A) - E_{A}^{\alpha}(A)] + [E_{AB}^{\beta}(B) - E_{B}^{\beta}(B)] \quad (4)$$

where the subscripts represent the geometries and the superscripts are the basis sets.[25−28] Specifically, $\alpha\cup\beta$ represents the basis set for dimer AB, while α and β are the basis sets for monomers A and B, respectively. For example, $E_A^{\alpha}(A)$ is the energy of monomer A whose geometry is that found in isolated monomer A (i.e., optimized A) and determined using that monomer's basis set. In comparison, $E_{AB}^{\alpha\cup\beta}(A)$ is the energy of monomer A whose geometry is that found in the AB dimer and determined using the dimer's basis set. Equations 2−4 represent the traditional, counter-poise,[25] and rigorous[26] approaches for computing the interaction energies. Equation 2 involves fully optimized geometries and unequal-sized basis functions. Equation 3 involves each species being modeled by equal-sized basis functions with the geometries found in their dimer configurations. Equation 4 represents a more rigorous attempt to include monomer relaxation terms that are not present in eq 3. Relaxation terms are typically small in weakly bonded systems; however, they become notable with increased nonbonded interaction strength or when their magnitude is comparable to the error from basis set incompleteness.[26] In this study, the basis set incompleteness is expected to be small when using aQZ, thus warranting the inclusion of eq 4.

Electronic interaction energies (ΔE_{el}) were corrected for basis set superposition error (BSSE) using counterpoise corrections[25] (see eq 3). Interaction Gibbs free energies ($\Delta G°$) were computed using CCSD(T)/CBS electronic energies, MP2/aQZ rotational constants, and scaled vibrational frequencies at a standard state pressure of 101.325 kPa. A Python script for computing statistical thermodynamic observables was used (https://github.com/m3-center/StatThermoPy.git). Boltzmann populations were computed from the ($\Delta G°$) values using specified temperatures.

PyMol was used to build input structures, visualize results, and render images.[29] The Symmetrizer algorithm was used to generate structures that conform to a specific point group.[30] Workflow scripts, algorithms, and plotting were written in Python (v.3.9), utilizing Matplotlib,[31] NumPy,[32] and Pandas.[33,34]

RESULTS

The optimized configurations of the BZ···MeOH dimer minima are shown in Figure 1. Configurations A1 and B2 have two alternate orientations—A1′ and B2′ (Figure S1)—that differ in how methanol's methyl group interacts with benzene. While the A′ configuration was optimized at the MP2/aTZ theory level, it could not be reproduced when using the other basis sets. The B2′ configuration was optimized by the unadjusted (i.e., default s_tolerance) MP2/aTZ theory level. Consequently, the primary focus herein will be on A1, B1, B2, and C1, all minima on the MP2/aQZ potential energy surface.

Table 2 presents the characteristic intermolecular distances for A1, B1, B2, and C1, with previously published distances provided in Table S1. These distances are metrics that

Table 2. Selected Intermolecular Distances (Å) from MP2 Full Optimizations and Experiment

	aTZ	aQZ	experiment[2]
	A1		
(C)−H···centroid[a]	3.554, 4.705	3.567, 4.722	
C···centroid	3.634	3.650	
(O)−H···centroid	2.290	2.320	2.30
O···centroid	3.222	3.247	3.35
	B1		
(C)−H···centroid[a]	2.422, 4.049	2.461, 4.084	
C···centroid	3.442	3.476	
(O)−H···centroid	4.683	4.702	
O···centroid	3.723	3.744	
	B2		
(C)−H···centroid[a]	2.544, 3.581	2.587, 3.599	
C···centroid	3.398	3.428	
(O)−H···centroid	5.316	5.347	
O···centroid	4.571	4.608	
	C1		
BZ−H···O[b]	2.631, 2.631	2.647, 2.647	2.9
BZ−H···H−(O)	3.440	3.452	
(C)−H···centroid[a]	3.532, 5.085	3.552, 5.101	
C···centroid	4.433	4.448	
(O)−H···centroid	5.271	5.278	
O···centroid	4.329	4.340	4.90

[a]The two distances represent the interactions arising from all three methyl hydrogens. [b]Each distance represents two equivalent interactions arising from a bifurcated BZ−H···O geometry.

https://doi.org/10.1021/acs.jpca.5c03923
J. Phys. Chem. A 2025, 129, 8110−8119

Table 3. Relative Electronic Energy (ΔE_{el}; kcal mol^{-1}) for Configurations of the BZ···MeOH Dimer

		MP2						
config	sym	aDZ[a]	aTZ	aQZ	CBS(a[DT]Z)[a]	CBS(a[TQ]Z)[a]	CBS(a[DTQ]Z)[a]	donor···acceptor
Basis Functions		274	595−596	1100				
A1	Cs	0.000	0.000	0.000	0.000	0.000	0.000	O−H···π
B1	Cs	1.987	1.998	1.970	2.146	1.956	1.920	CH_3···π
B2	Cs	2.468	2.355	2.270	2.553	2.276	2.235	CH_3···π
C1	Cs	2.892	2.118	1.867	2.383	1.957	1.914	Bz−H···O

	CCSD(T)					
	aDZ[a]	aTZ[a]	aQZ[a]	CBS(a[DT]Z)[a]	CBS(a[TQ]Z)[a]	CBS(a[DTQ]Z)[a]
A1	0.000	0.000	0.000	0.000	0.000	0.000
B1	2.015	2.083	1.968	2.107	1.917	1.880
B2	2.329	2.331	2.149	2.343	2.057	2.016
C1	2.599	1.981	1.627	1.853	1.443	1.400

[a]Energies were computed using the MP2/aQZ fully optimized geometries.

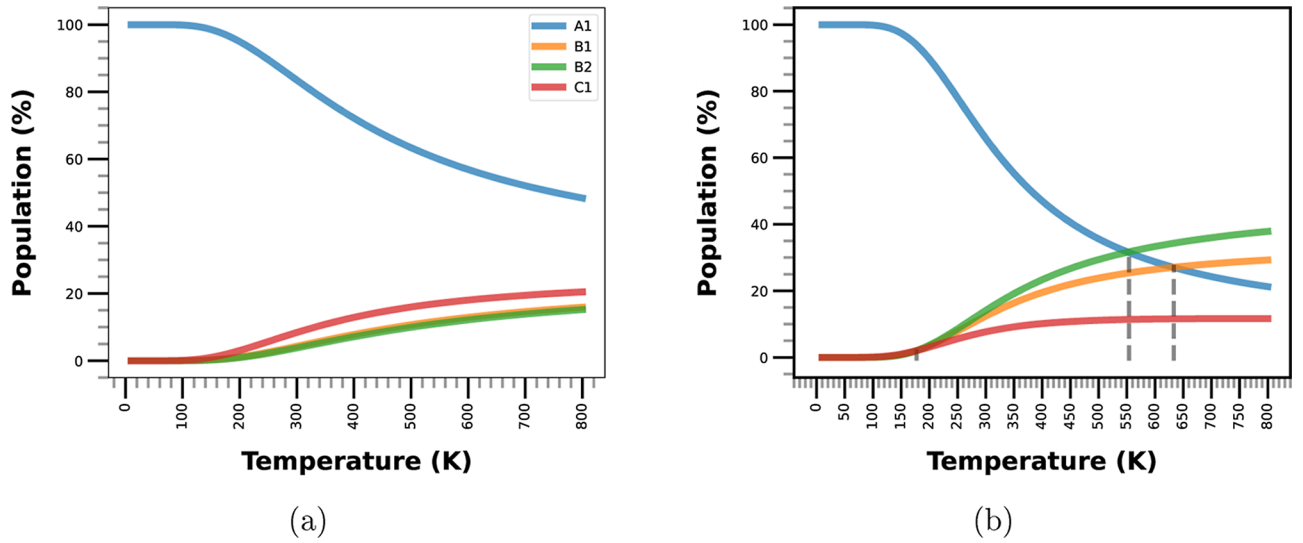

Figure 2. CCSD(T)/CBS(a[DTQ]Z)//MP2/aQZ Boltzmann populations of BZ···MeOH configurations as a function of temperature using (a) ΔE_{zpve} and (b) $\Delta G°$ relative energies. The intersection points where configurations have the same $\Delta G°$ stability are highlighted with dashed lines for B1, B2, and C1 (T = 177 K); A1 and B2 (T = 554 K); and A1 and B1 (T = 633 K).

Table 4. Gibbs Relative Free Energies ($\Delta G°$; kcal mol^{-1}) and Boltzmann Population (%) in Parentheses at Various Temperatures for Configurations of the Benzene···Methanol Dimer[a]

	$\Delta G°$					
temperature (K)	10.0	177.0	298.15	554.0	633.0	800.0
A1	0.00 (100)	0.00 (94)	0.00 (66)	**0.00** (32)	**0.30** (27)	0.92 (21)
B1	1.81 (0)	**1.35** (2)	1.00 (12)	0.24 (25)	**0.30** (27)	0.41 (29)
B2	1.87 (0)	**1.35** (2)	0.93 (14)	**0.00** (32)	0.00 (34)	0.00 (38)
C1	1.39 (0)	**1.35** (2)	1.28 (8)	1.13 (11)	1.37 (12)	1.88 (12)

[a]Free energies were computed at a standard state pressure of 101.325 kPa, CCSD(T)/CBS(a[DTQ]Z) ΔE_{el}, and scaled MP2/aQZ frequencies. Bold-faced values are when configurations have equal $\Delta G°$.

experimentalists might use for comparison in their studies. This includes different MeOH atom distances to BZ's centroid for the A1, B1, and B2 out-of-plane configurations and the BZ hydrogen to MeOH oxygen distance for the C1 in-plane configuration. The optimized coordinates of these structures are provided in the Supporting Information.

The configurations' relative stabilities—computed from electronic energies (ΔE_{el})—are provided in Table 3, calculated at theory levels ranging from MP2/aDZ//MP2/aQZ to CCSD(T)/CBS(a[DTQ]Z)//MP2/aQZ. For both MP2 and CCSD(T), the stability range is the smallest when using the most robust basis set extrapolation (e.g., CCSD(T)/CBS(a-[DTQ]Z) = 0.00−2.02 kcal mol^{-1}) and largest when using the smallest basis set (e.g., MP2/aDZ = 0.00−2.89 kcal mol^{-1}).

Based on the relative stabilities, Boltzmann populations were computed using zero-point vibration-corrected energies (ΔE_{zpve}) and Gibbs free energies ($\Delta G°$) at standard pressure. Figure 2 shows the predicted ΔE_{zpve} and $\Delta G°$ population over a temperature range of 10−850 K, whose selected values are given in Tables S2 and 4, respectively. In the absence of pressure and

https://doi.org/10.1021/acs.jpca.5c03923
J. Phys. Chem. A 2025, 129, 8110−8119

Table 5. Electronic Interaction Energy (ΔE_{el}; kcal mol^{-1}) for Configurations of the BZ···MeOH Dimer, Computed with (ΔE_{CP}, eq 3) and without (ΔE, eq 2) Counterpoise Correction, as well as Including Monomer Relaxation Energies (ΔE_{Rig}, eq 4)[a]

	MP2					
	aDZ	aTZ	aQZ	CBS(a[DT]Z)	CBS(a[TQ]Z)	CBS(a[DTQ]Z)
equation	ΔE_{CP} (ΔE)	ΔE_{CP} (ΔE)	ΔE_{CP} (ΔE)	ΔE_{CP} (ΔE)	ΔE_{CP} (ΔE)	ΔE_{CP} (ΔE)
A1	−3.863 (−6.898)	−4.508 (−5.781)	−4.667 (−5.131)	−4.765 (−5.642)	−4.782 (−4.783)	−4.780 (−4.735)
B1	−2.225 (−4.911)	−2.649 (−3.679)	−2.768 (−3.132)	−2.823 (−3.496)	−2.853 (−2.826)	−2.853 (−2.815)
B2	−2.005 (−4.431)	−2.337 (−3.261)	−2.435 (−2.776)	−2.489 (−3.089)	−2.505 (−2.506)	−2.511 (−2.500)
C1	−2.360 (−4.007)	−2.658 (−3.341)	−2.757 (−3.012)	−2.808 (−3.259)	−2.829 (−2.825)	−2.835 (−2.821)
	CCSD(T)					
	aDZ	aTZ	aQZ	aQZ	CBS(a[DT]Z)	CBS(a[TQ]Z)	CBS(a[DTQ]Z)
equation	ΔE_{CP} (ΔE)	ΔE_{CP} (ΔE)	ΔE_{CP} (ΔE)	ΔE_{Rig}	ΔE_{CP} (ΔE)	ΔE_{CP} (ΔE)	ΔE_{CP} (ΔE)
A1	−3.208 (−6.422)	−3.843 (−5.085)	−3.985 (−4.368)	−3.980	−4.098 (−4.854)	−4.088 (−3.971)	−4.086 (−3.923)
B1	−1.590 (−4.407)	−2.006 (−3.002)	−2.107 (−2.400)	−2.096	−2.176 (−2.747)	−2.180 (−2.054)	−2.180 (−2.043)
B2	−1.543 (−4.093)	−1.856 (−2.754)	−1.939 (−2.219)	−1.948	−2.000 (−2.511)	−1.997 (−1.914)	−2.003 (−1.907)
C1	−2.109 (−3.823)	−2.438 (−3.104)	−2.530 (−2.741)	−2.513	−2.601 (−3.000)	−2.598 (−2.528)	−2.603 (−2.523)

[a]All energies were computed on the MP2/aQZ fully optimized geometries.

Table 6. Gibbs Interaction Free Energies ($\Delta G°$; kcal mol^{-1}) at Various Temperatures for Configurations of the Benzene··· Methanol Dimer[a]

temperature (K)	10.0	71.0	82.0	143.0	177.0	298.15	554.0	633.0	800.0
A1	−3.14	−1.67	−1.41	**0.02**	0.78	3.32	**8.16**	**9.55**	12.37
B1	−1.38	**−0.03**	0.21	1.47	**2.13**	4.32	8.40	**9.55**	11.86
B2	−1.31	**0.03**	0.26	1.49	**2.13**	4.25	**8.15**	9.15	11.45
C1	−1.77	−0.28	**−0.01**	1.39	**2.13**	4.61	9.28	10.62	13.33

[a]Free energies were computed at a standard state pressure of 101.325 kPa, using CCSD(T)/CBS(a[DTQ]Z)//MP2/aQZ electronic energies and scaled MP2/aQZ frequencies.

entropy influences, A1 is the dominant configuration throughout the temperature range (Figure 2a). However, when the standard pressure and entropy are considered, a different population profile is observed (Figure 2b). As the temperature increases, the B1, B2, and C1 configurations become increasingly populated. At predicted temperatures of 554 and 633 K, B2 and B1 equal A1's relative energy, and subsequently at higher temperatures, they become the most populated.

Predicted ΔE_{el} interaction energies for the configurations are shown in Table 5, whose values were computed by using the MP2/aQZ optimized geometries (e.g., MP2/aDZ//MP2/aQZ). The use of MP2/aQZ geometries allows for a consistent comparison of how the basis set size affects the energies. As observed in previous studies,[3,9,10] correcting for BSSE has a significant influence on the interaction energies. Generally, the magnitude of the BSSE corrections follows the configuration trend of A1 > B1 > B2 > C1. Correcting for monomer relaxation using eq 4 alters the interaction energies negligibly due to weak intermolecular forces. Extrapolating to the CBS limit further converges the interaction energies. Interestingly, the use of the CP-corrected energies in the extrapolation shows very close agreement when extrapolations were done using the a[DT]Z, a[TQ]Z, and a[DTQ]Z basis sets, while non-CP-corrected energies show notable a[DT]Z variance. This is attributed to the larger orbital space used in computing the monomer energies within the CP correction. For illustration, when using eq 2, the number of basis functions for the BZ and MeOH monomers (i.e., α and β) are 414 and 184, respectively, when considering the aTZ basis set. However, when using the CP correction of eq 3, the number of basis functions increases to 598 for each monomer due to the union of the basis functions present in both of them (i.e., $\alpha \cup \beta$). This larger number of monomer functions present when using eq 3 better corrects for the basis set incompleteness compared to that when using eq 2.

CCSD(T)/CBS(a[DTQ]Z) interaction $\Delta G°$ were computed from 10 to 850 K in 10 K increments, as shown in Figure S2. A second-degree polynomial was fitted to these data whose coefficients of determination (i.e., R^2) were all 0.9998(1), indicating excellent data reproduction. The intersection points of the polynomials and the temperatures where the $\Delta G° \approx 0$ kcal mol^{-1} were subsequently computed. The intersection temperatures of the polynomial curves occur at approximately 172 (i.e., $\Delta G°_{172K}(B1) = \Delta G°_{172K}(B2)$), 176 (i.e., $\Delta G°_{176K}(B2) = \Delta G°_{176K}(C1)$), 177 (i.e., $\Delta G°_{177K}(B1) = \Delta G°_{177K}(C1)$), 554 (i.e., $\Delta G°_{565K}(A1) = \Delta G°_{565K}(B2)$), and 633 K (i.e., $\Delta G°_{633K}(A1) = \Delta G°_{633K}(B1)$). The temperatures when $\Delta G° \approx 0.0$ kcal mol^{-1} are approximately 143, 71, and 82 K for A1, B1 ≈ B2, and C1, respectively. The $\Delta G°$ interaction energies at these temperatures are provided in Table 6.

Two scaling factor values were optimized using the combined monomer frequencies—one for low and one for high vibrations using a 1000 cm^{-1} cutoff criteria, as done by Wilson and coworkers.[35] These factors were obtained by fitting the unscaled MP2/aQZ frequencies to their corresponding experimental values,[22,23,36−44] whose values (along with published CCSD(T)[45,46]) are provided in Tables S3 and S4. The resulting optimized low and high scaling factors were 0.9911 and 0.9523, respectively. Using these scaling factors, Table 7 presents the dimers and the monomers' scaled MP2/aQZ vibrations, with the unscaled dimer frequencies given in Table S5.

DISCUSSION

Since 1990, several groups (Table 1) have studied the BZ··· MeOH dimer.[2,3,6−8,10,47,48] The consensus of these studies is

https://doi.org/10.1021/acs.jpca.5c03923
J. Phys. Chem. A 2025, 129, 8110−8119

Table 7. MP2/aQZ and Experimental Vibrational Frequencies (cm^{-1}) for BZ···MeOH[c]

	Dimers				Monomers		
	A1	B1	B2	C1	BZ & MeOH	Experiment[a]	Description
1	6	10	5	21			intermolecular
2	46	11	32	29			intermolecular
3	46	47	39	41			intermolecular
4	88	61	72	64			intermolecular
5	112	97	83	86			intermolecular
6	114	132	86	112			intermolecular
7	**335**	306	302	305	293	271.5[23]	OH wag
8	402	400	401	405	399	398.133[42]	e_{2u}
9	404	401	401	406			
10	602	602	602	601	603	608.13[43]	e_{2g}
11	602	602	602	604			
12	687	682	682	692	683	673.97465[43]	a_{2u}
13	**699**	**696**	**696**	**699**	667	702.24[44]	b_{2g}
14	861	855	857	859	854	847.1062[43]	e_{1g}
15	862	856	858	867			
16	978	973	975	978	968	967.98[44]	e_{2u}
17	979	974	975	979			
18	960	958	959	966	965	992.93[44]	b_{2g}
19	963	963	964	963	965	993.071[36]	a_{1g}
20	976	976	975	974	973	1013.74[44]	b_{1u}
21	1010	1010	1010	1008	1011	1038.267[39]	e_{1u}
22	1011	1011	1011	1011			
23	1019	1003	1004	1005	1010	1033.5[23]	ν CO
24	1048	1037	1035	1038	1041	1076.5[23]	δ CH rock + δ HOC
25	1114	1113	1113	1111	1113	1147.6751[43]	b_{2u}
26	1129	1128	1127	1129	1130	1145.0[b][23]	δCH_3 wag
27	1139	1139	1139	1137	1139	1177.776[42]	e_{2g}
28	1139	1139	1139	1137			
29	1307	1306	1306	1304	1304	1350[22]	a_{2g}
30	1315	1304	1303	1305	1308	1334.0[23]	δ COH
31	1389	1392	1391	1388	1388	1309.4[41]	b_{2u}
32	1414	1416	1412	1419	1420	1451.5[23]	δ_{sym} HCH
33	1434	1434	1435	1433	1435	1483.9854[38]	e_{1u}
34	1434	1435	1435	1434			
35	1443	1446	1441	1452	1451	1466.0[23]	δ_{asym} HCH
36	1455	1457	1456	1458	1461	1473.0[23]	δ_{asym} HCH
37	1556	1558	1558	1558	1560	1609.518[40]	e_{2g}
38	1557	1558	1558	1558			
39	2898	2907	2906	2913	2912	2847.5[23]	ν_{sym} CH
40	2965	2977	2977	2984	2982	2961.5[23]	ν_{asym} CH
41	3023	3040	3038	3036	3038	3005.5[23]	ν_{asym} CH
42	3050	3047	3047	3045	3047	3057[22]	b_{1u}
43	3060	3057	3057	3055	3057	3057.04[44]	e_{2g}
44	3060	3060	3057	3060			
45	3074	3071	3071	3071	3071	3047.908[37]	e_{1u}
46	3075	3072	3072	3072			
47	3084	3083	3080	3080	3082	3073.942[36]	a_{1g}
48	**3635**	3681	3691	3686	3693	3667.0[23]	ν OH

[a]Experimental values for MeOH were obtained in an argon matrix at 15 K, with one noted exception. [b]Value obtained in the vapor phase at ca. 300 K and ca. 0.01 bar. [c]The MP2/aQZ frequencies below and above 1000 cm^{-1} have been scaled by 0.9911 and 0.9523, respectively. Notable red- and blue-shifted frequencies (i.e., $|\Delta| \geq 9$ cm^{-1}) are color-coded, with prominent values (i.e., $|\Delta| \geq 29$ cm^{-1}) given in boldface. For the BZ monomer, only a single frequency value is provided for the degenerate vibrational modes (i.e., e_{1u}, e_{2u}, and e_{2g}).

that the O−H···π interaction is the most stable configuration (Figure 1 and Table S6). However, depending on the theory level (e.g., MP2/6-31+G(d,p), B3LYP/6-31+G(d), and M06-2X/6-31++G(d,p)), differing configurations were found to be minima on their respective potential energy surfaces. For illustration, Matisz et al. reported the existence of three possible interaction configurations: A1′, B2″, and C1.[3] The B2″ configuration (Figure S1) was optimized using the M06-2X/6-31+G(d,p) theory but not when employing MP2/6-31+G(d,p). Interestingly, in a limited exploration of different basis sets, we were able to optimize the B2″ structure only at the MP2/def2-TZVPD theory level. Another unique but questionable structure was optimized by B3LYP/6-31+G(d), which has an out-of-plane O−H···π orientation where the alcohol hydrogen is directed toward a C≡C bond.[7] Since these structures were not found again using larger basis sets or by non-DFT approaches, they are likely artifacts.

Lacking in the literature is a comprehensive study of BZ···MeOH's configurations. Collected from the different published configurations, either directly from the Supporting Information or by attempted reproduction of geometries shown in figures, we attempted to optimize them at the MP2 theory level. While the data are not fully provided, we can confirm that different configurations were found when using smaller basis sets that included aDZ and selected Karlsruhe basis sets. For example, the most minima (5 in total) were found using the def2-TZVPD basis set. However, employing the two largest basis sets, aTZ and aQZ, we consistently found only the following four config-

https://doi.org/10.1021/acs.jpca.5c03923
J. Phys. Chem. A 2025, 129, 8110−8119

urations as minima: one O−H···π (A1), two CH_3···π (B1 and B2), and one Bz−H···O (C1) (Figure 1).

Geometries. Di Mino et al. recently reported a solution-phase H/D isotopic substitution neutron diffraction study that revealed strong out-of-plane O−H···π interactions (A1), where the hydroxyl hydrogen and oxygen are, respectively, 2.30 and 3.25 Å from BZ's centroid.[2] Despite the difference in phases, the MP2 optimizations using aTZ and aQZ basis sets reproduce the A1 geometry very well (Table 2), with corresponding distances of 2.29 and 2.32 Å for the (O)−H···centroid and for 3.22 and 3.25 Å for the O···centroid. The computed distances for the other configurations yield a (O)−H···centroid distance of ≥4.7 Å, clearly confirming the experimental presence of the A1 configuration.

The experimental data also indicate that the in-plane configuration (C1) is populated, with the BZ−H···O and O··· centroid distances of 2.9 Å and 4.90 Å, respectively.[2] The experimental data were interpreted to have methanol's O and H atoms both lying in the plane formed by the BZ ring, with a BZ−H···O bifurcated interaction. Consequently, methanol's hydroxyl hydrogen atom would be positioned in close proximity to BZ's H. This geometry was not observed in the current and previous studies (Table S1), where the predicted BZ−H···O distances for C1 were significantly smaller (2.14−2.65 Å) than the experimental value, a trend that is mirrored in the O···centroid distance. In the gas-phase QM predictions, the hydroxyl hydrogen is pointed away from BZ (Figure 1). Nevertheless, the experiment and the MP2 optimizations using the aTZ and aQZ basis sets all identify a BZ−H···O bifurcated interaction.

Not addressed in the experimental study were the less stable out-of-plane B1 and B2 configurations. MP2/aQZ results show similar C···centroid distances of 3.48 and 3.43 Å but differ in their O···centroid distances of 3.74 and 4.61 Å. Interestingly, if we consider the relative $\Delta G°$ energies (Table 4) at 298.15 K, a temperature close to the experimental 273 K value, B1 and B2 are predicted to be slightly more populated than C1 in the gas phase.

Relative Stability. For all theory levels studied herein, A1 was the most stable configuration when comparing ΔE_{el} (Table 3). When using the MP2 theory, the predicted stability ordering is dependent upon the basis set size, where aDZ and aTZ predict A1 > B1 > C1 > B2, while aQZ predicts A1 > C1 > B1 > B2. Extrapolating to the CBS, MP2/CBS(a[TQ]Z), and MP2/CBS(a[DTQ]Z) theory levels, the predicted stability becomes A1 > C1 ≈ B1 > B2. Concerning the CCSD(T) theory, the trend is slightly different, with aQZ and the CBS extrapolations firmly predicting A1 > C1 > B1 > B2. The overall data trends indicate that the ΔE_{el} relative stability of B1 and C1 is sensitive to the molecular orbital modeling, requiring a very large description of their space and rigorous electron correlation modeling.

Using the scaled MP2/aQZ vibrational frequencies and adjusting the CBS(a[DTQ]Z) ΔE_{el} for ZPV energy, the ordering remains the same, with relative ΔE_{zpve} stabilities of 0.00 (A1), 1.37 (C1), 1.77 (B1), and 1.84 (B2) kcal mol^{-1} (Table S2). The ΔE_{zpve} values represent the best predicted relative configuration energies for isolated dimers at very low temperatures. A Boltzmann distribution analysis showed the A1 configuration to be 100% populated at temperatures below ca. 143 K (Figure 2a and Table S2).

Adjusting the relative energies to account for standard pressure and vibrational entropy effects, the stability trend changes, revealing an interesting temperature dependency (Figure 2b and Table 4). As the temperature increases, the relative stabilities of B1 and B2 notably increase at the expense of A1. The C1 configuration, which was the second most stable dimer when considering ΔE_{zpve} at low temperatures, becomes the overall least stable starting at an estimated 177 K. At approximately 554 K, B2 becomes the most stable configuration, while near 633 K, B1 becomes more stable than A1. It should be noted that the indicated temperatures are approximate, as their values arise from CBS extrapolations, polynomial fittings, and scaling factor adjustments of harmonic frequencies. Nevertheless, the general free energy trends observed as a function of the temperature should be reliable.

Interaction Energies. CCSD(T)/CBS computations (i.e., CBS(a[DT]Z), CBS(a[TQ]Z), and CBS(a[DTQ]Z) using CP-corrected energies in the extrapolations) predicted electronic interaction energies (ΔE_{el}) of −4.09, −2.18, −2.00, and −2.60 kcal mol^{-1} for A1, B1, B2, and C1, respectively (Table 5). In comparison, the interaction energies are consistently overestimated at the MP2 theory level.[49,50] Both MP2 and CCSD(T) calculations consistently predict the A1's O−H···π interaction to have the strongest interaction energy.

Previous studies reported interaction energies that focused on the O−H···π and Bz−H···O motifs, giving values ranging from −0.79 to −5.45 and −1.89 to −2.89 kcal mol^{-1} (Table S6), respectively.[3,6,7,9,10] Of these studies, the most rigorous theoretical level, BSSE-corrected CCSD(T)/aTZ//MP2/aDZ, yielded interaction energies of −4.02 and −2.51 kcal mol^{-1} for A1 and C1, respectively, where the CCSD(T) correction term was computed from CCSD(T) and MP2 calculations using the smaller DZ basis set.[6] These values agree well with our CCSD(T)/CBS//MP2/aQZ values of −4.09 and −2.60 kcal mol^{-1}. MP2/CBS extrapolations, with BSSE corrections computed at MP2/6-31+G(d,p) geometries, were also previously performed, yielding interaction energies ranging from −4.68 to −4.76 for A1 and −2.70 to −2.75 kcal mol^{-1} for C1.[3] Our MP2/CBS(a[DTQ]Z)//MP2/aQZ results predict slightly more stable interactions at −4.78 and −2.84 kcal mol^{-1}. A literature search did not reveal the previously predicted interaction energies for B1 and B2. Our CCSD(T)/CBS values of −2.18 and −2.00 kcal mol^{-1} predict these configurations to be the weakest BZ and MeOH interactions.

Adjusting the interaction energy for temperature, zero-point vibration, and entropy revealed that all configurations will spontaneously form at very low temperatures (e.g., 10 K; Table 6). At a predicted temperature of approximately 71 K, only the spontaneous formation of A1 and C1 would occur, while at approximately >143 K, all configurations become unlikely in the gas phase.

Vibrational Frequencies. In comparison to the experimental frequencies, the unscaled harmonic MP2/aQZ values for the BZ and MeOH monomers have mean absolute error (MAE) values of 52 and 90 cm^{-1}, respectively. To account for anharmonicity and the electronic approximations inherent to the MP2/aQZ theory level, the following two experimentally targeted scaling adjustments were considered: (1) using broadly optimized scaling factors that were determined from many diverse molecules[20,35] or (2) target-optimized scaling factors that focus on specific molecules (i.e., BZ and MeOH). As expected, using the target-optimized scaling factors improved the frequencies to MAE values of 26 and 27 cm^{-1}, while the broadly optimized MP2/aQZ scaling factors published by Sinha et al. (low = 1.0698 and high = 0.9601)[35] resulted in MAE values of 41 and 31 cm^{-1}, respectively. Note that the Sinha et al. scaling

https://doi.org/10.1021/acs.jpca.5c03923
J. Phys. Chem. A 2025, 129, 8110−8119

factors were optimized using 41 organic molecules, which included BZ and MeOH.[51]

Given the good agreement obtained when applying the target-optimized scaling factors to the monomers and considering that the dimer formation should induce small geometry perturbations in the constituent monomers, the frequencies for the four BZ···MeOH dimer configurations in Table 7 represent the best predicted values. The formation of a dimer results in 6 new low intermolecular modes, all lower than the lowest monomer vibration (i.e., the OH wag at 271.5 cm^{-1}). Due to their greater anharmonic nature, these frequencies are likely less accurately predicted. The remaining dimer frequencies all follow the monomer modes, with very slight perturbations in their values: for A1, B1, B2, and C1, a mean absolute difference of 8, 4, 3, and 4 cm^{-1} are obtained, respectively, when comparing the scaled MP2/aQZ dimer and monomer frequencies.

All dimers manifest a 9−42 cm^{-1} blueshift in the OH wag mode and a 29−32 blueshift in the lowest b_{2g} mode. The A1 dimer formation results in the most notable frequency shifts, with the largest being a 58 cm^{-1} redshift in the OH stretching vibration, 14−17 cm^{-1} redshifts in methanol's CH stretching, and a possibly detectable unique blueshift (9 cm^{-1}) in the CO stretch vibration. Through resonant ion-dip infrared spectroscopy by Zwier and co-workers, A1's OH and two CH stretching redshifts were observed, with values of 42, 7.9, and 12.9 cm^{-1}, respectively.[7,8] Note that in those publications, the B3LYP/6-31+G(d) theory was used for comparison to the experimental data, which proposed an A1 geometry where MeOH's alcohol group is interacting with a BZ C=C bond and the methyl group showing little interaction with BZ. Conversely, the MP2/aQZ geometries have the alcohol group directed toward the centroid and the methyl group closer to the ring.

Unique to the second most stable dimer formation −C1− is a very slight blueshift (9 cm^{-1}) in an a_{2u} mode. The two less stable dimers, B1 and B2, do not manifest any unique frequency shift upon formation. Taken collectively, the small shifts that manifest uniquely in the dimer formations and the general overlap of the stronger shift would make resolving B1, B2, and C1 individually very difficult.

Additional Comment on Eigenvalue Overlap. In 2006, it was observed that several Pople basis sets incorrectly modeled aromatic hydrocarbons when used with electron-correlated theories.[52] In 2017, Samala and Jordan also showed that D_{6h} benzene, when optimized using MP2 and the Dunning aTZ basis set, results in an imaginary b_{2g} vibration mode (493*i* cm^{-1}).[53] This occurs due to the basis set's near-linear dependency, specifically when all of the overlap eigenvectors (i.e., molecular orbitals) are retained in the calculation. This result was confirmed in our MP2/aTZ results (ca. 491*i* cm^{-1}) for D_{6h} benzene (using the full set of 414 basis functions), while the C_1 benzene optimization gave a structure whose frequencies were all real. Following the suggestion of Samala and Jordan, a tolerance reduction of the overlap eigenvalue from Psi4's default value of 1×10^{-7} to 1×10^{-6} resulted in removing two molecular orbitals and all positive frequencies.

Furthermore, MP2/aTZ, with the default overlap eigenvalue tolerance, optimized to two B2 minima, whose configurations differ in how methanol's methyl hydrogens interact with benzene (B2 in Figure 1 and B2′ in Figure S1). Reducing the overlap eigenvalue criteria to 1×10^{-6} resulted in only the B2 minima being optimized. Given the conclusions from the isolated benzene study, we believe that MP2/aTZ with a 1×10^{-6} criterion is the better model of the dimer system, which is in agreement with the MP2/aQZ optimizations.

CONCLUSION

Understanding the strength and geometry of nonbonded interactions is important for many research fields (e.g., atmospheric chemistry and biology). O−H···π is one such fundamental interaction which can be exemplified by the BZ···MeOH dimer. This paper presents a rigorous QM investigation of this dimer, predicting the relative stabilities, electronic and Gibbs free interaction energies, and vibrational frequencies of four distinct configurations: O−H···π (A1), CH_3···π (B1, B2), and Bz−H···O (C1) (Figure 1).

The CCSD(T)/CBS theory established the O−H···π (A1) configuration as the most stable at low temperatures, with an electronic interaction energy of −4.09 kcal mol^{-1}. The CH_3···π (B1, B2) and Bz−H···O (C1) configurations were predicted to be less stable by 1.40−2.02 kcal mol^{-1}, with interaction energies between 2.00 and 2.60 kcal mol^{-1}. The MP2/aQZ optimized geometry of A1 is in good agreement with the recent experimental neutron diffraction data, while the theoretical and experimental structures for C1 show differences. However, the common theory and experimental result for C1 are that the Bz−H···interaction is bifurcated.

Using scaled frequencies, the temperature dependence of the configurations' relative stabilities was also investigated. While the A1 configuration dominates at low temperatures, Gibbs free energy calculations revealed that the CH_3···π configurations (B1 and B2) become more stable and populated as the temperature increases. An examination of how vibrational frequency shifts occur in each configuration revealed that the O−H···π (A1) configuration exhibits the most notable changes, consistent with previous spectroscopic observations. The shifts computed in the other configurations suggest that it is likely to be very difficult to experimentally observe them.

ASSOCIATED CONTENT

Supporting Information

The Supporting Information is available free of charge at https://pubs.acs.org/doi/10.1021/acs.jpca.5c03923.

Previously published structural and interaction energy data; ΔE_{zpve}-corrected relative energies and populations; plot of interaction $\Delta G°$ values at differing temperatures; MP2/aQZ unscaled and scaled frequencies for monomers (including previously published CCSD(T) and experimental values) and dimers; and MP2 data computed using additional basis sets (PDF)

XYZ-formatted file containing MP2/aQZ optimized structures of A1, B1, B2, and C1 (XYZ)

AUTHOR INFORMATION

Corresponding Author

Karl N. Kirschner − *Department of Computer Science and the Institute of Technology, Resource and Energy-Efficient Engineering (TREE), University of Applied Sciences Bonn-Rhein-Sieg, Sankt Augustin 53757, Germany;* orcid.org/0000-0002-4581-920X; Email: karl.kirschner@h-brs.de

Complete contact information is available at: https://pubs.acs.org/10.1021/acs.jpca.5c03923

Notes

The author declares no competing financial interest.

■ ACKNOWLEDGMENTS

This work was partially supported by the German Research Foundation (DFG, Deutsche Forschungsgemeinschaft) Project-ID 528562393—FIP 26. The author thanks Rudolf Berrendorf and Javed Razzaq for their continuous development and support of the BRSU's computing cluster. The BRSU's computer hardware was supported by the Federal Ministry for Education and Research and by the Ministry for Innovation, Science, Research, and Technology of the state North Rhine-Westfalia (grant 13FH156IN6).

■ REFERENCES

(1) Kim, K. S.; Tarakeshwar, P.; Lee, J. Y. Molecular Clusters of π-Systems: Theoretical Studies of Structures, Spectra, and Origin of Interaction Energies. *Chem. Rev.* **2000**, *100*, 4145−4186.
(2) Di Mino, C.; Seel, A. G.; Clancy, A. J.; Headen, T. F.; Földes, T.; Rosta, E.; Sella, A.; Skipper, N. T. Strong Structuring Arising from Weak Cooperative O-H···π and C-H···O Hydrogen Bonding in Benzene-methanol Solution. *Nat. Commun.* **2023**, *14*, 5900.
(3) Matisz, G.; Kelterer, A.-M.; Fabian, W. M. F.; Kunsági-Máté, S. Coordination of Methanol Clusters to Benzene: A Computational Study. *J. Phys. Chem. A* **2011**, *115*, 10556−10564.
(4) Řezáč, J.; Riley, K. E.; Hobza, P. S66: A Well-balanced Database of Benchmark Interaction Energies Relevant to Biomolecular Structures. *J. Chem. Theory Comput.* **2011**, *7*, 2427−2438.
(5) Řezáč, J.; Riley, K. E.; Hobza, P. Erratum to "S66: A Well-balanced Database of Benchmark Interaction Energies Relevant to Biomolecular Structures". *J. Chem. Theory Comput.* **2014**, *10*, 1359−1360.
(6) Marchione, D.; McCoustra, M. R. S. Non-covalent interaction of benzene with methanol and diethyl ether solid surfaces. *Phys. Chem. Chem. Phys.* **2016**, *18*, 20790−20801.
(7) Pribble, R. N.; Hagemeister, F. C.; Zwier, T. S. Resonant ion-dip infrared spectroscopy of benzene-(methanol)m clusters with m = 1−6. *J. Chem. Phys.* **1997**, *106*, 2145−2157.
(8) Gruenloh, C. J.; Florio, G. M.; Carney, J. R.; Hagemeister, F. C.; Zwier, T. S. C−H Stretch Modes as a Probe of H-Bonding in Methanol-Containing Clusters. *J. Phys. Chem. A* **1999**, *103*, 496−502.
(9) Buchhold, K.; Reimann, B.; Djafari, S.; Barth, H.-D.; Brutschy, B.; Tarakeshwar, P.; Kim, K. S. Fluorobenzene and p-difluorobenzene microsolvated by methanol: An infrared spectroscopic and ab initio theoretical investigation. *J. Chem. Phys.* **2000**, *112*, 1844−1858.
(10) Pankewitz, T.; Klopper, W. Ab Initio Modeling of Methanol Interaction with Single-Walled Carbon Nanotubes. *J. Phys. Chem. C* **2007**, *111*, 18917−18926.
(11) Dunning, T. H. Gaussian basis sets for use in correlated molecular calculations. I. The atoms boron through neon and hydrogen. *J. Chem. Phys.* **1989**, *90*, 1007−1023.
(12) Halkier, A.; Helgaker, T.; Jørgensen, P.; Klopper, W.; Koch, H.; Olsen, J.; Wilson, A. K. Basis-set convergence in correlated calculations on Ne, N_2, and H_2O. *Chem. Phys. Lett.* **1998**, *286*, 243−252.
(13) Halkier, A.; Helgaker, T.; Jørgensen, P.; Klopper, W.; Olsen, J. Basis-set convergence of the energy in molecular Hartree-Fock calculations. *Chem. Phys. Lett.* **1999**, *302*, 437−446.
(14) Feyereisen, M.; Fitzgerald, G.; Komornicki, A. Use of approximate integrals in ab initio theory. An application in MP2 energy calculations. *Chem. Phys. Lett.* **1993**, *208*, 359−363.
(15) Rendell, A. P.; Lee, T. J. Coupled-cluster theory employing approximate integrals: An approach to avoid the input/output and storage bottlenecks. *J. Chem. Phys.* **1994**, *101*, 400−408.
(16) Weigend, F. A fully direct RI-HF algorithm: Implementation, optimized auxiliary basis sets, demonstration of accuracy and efficiency. *Phys. Chem. Chem. Phys.* **2002**, *4*, 4285−4291.
(17) Weigend, F.; Köhn, A.; Hättig, C. Efficient use of the correlation consistent basis sets in resolution of the identity MP2 calculations. *J. Chem. Phys.* **2002**, *116*, 3175−3183.
(18) Werner, H.-J.; Manby, F. R.; Knowles, P. J. Fast linear scaling second-order Møller-Plesset perturbation theory (MP2) using local and density fitting approximations. *J. Chem. Phys.* **2003**, *118*, 8149−8160.
(19) DePrince, A. E. I. I. I.; Sherrill, C. D. Accuracy and Efficiency of Coupled-Cluster Theory Using Density Fitting/Cholesky Decomposition, Frozen Natural Orbitals, and a t_1-Transformed Hamiltonian. *J. Chem. Theory Comput.* **2013**, *9*, 2687−2696.
(20) Scott, A. P.; Radom, L. Harmonic Vibrational Frequencies: An Evaluation of Hartree−Fock, Møller−PlessetPlesset, Quadratic Configuration Interaction, Density Functional Theory, and Semiempirical Scale Factors. *J. Phys. Chem.* **1996**, *100*, 16502−16513.
(21) Virtanen, P.; Gommers, R.; Oliphant, T. E.; Haberland, M.; Reddy, T.; Cournapeau, D.; Burovski, E.; Peterson, P.; Weckesser, W.; Bright, J.; et al. SciPy 1.0: fundamental algorithms for scientific computing in Python. *Nat. Methods* **2020**, *17*, 261−272.
(22) Brodersen, S.; Langseth, A. *The Infrared Spectra of Benzene, Symbenzene-d3, and Benzene-d6*; Munksgaard, 1956.
(23) Serrallach, A.; Meyer, R.; Günthard, H. H. Methanol and deuterated species: Infrared data, valence force field, rotamers, and conformation. *J. Mol. Spectrosc.* **1974**, *52*, 94−129.
(24) Miani, A.; Cané, E.; Palmieri, P.; Trombetti, A.; Handy, N. C. Experimental and theoretical anharmonicity for benzene using density functional theory. *J. Chem. Phys.* **2000**, *112*, 248−259.
(25) Boys, S.; Bernardi, F. The calculation of small molecular interactions by the differences of separate total energies. Some procedures with reduced errors. *Mol. Phys.* **1970**, *19*, 553−566.
(26) Xantheas, S. S. On the importance of the fragment relaxation energy terms in the estimation of the basis set superposition error correction to the intermolecular interaction energy. *J. Chem. Phys.* **1996**, *104*, 8821−8824.
(27) Rayón, V. M.; Sordo, J. A. On the validity of the counterpoise correction for the basis set superposition error including the fragment relaxation terms. *Theor. Chem. Acc.* **1998**, *99*, 68−70.
(28) Bowen, J. P.; Sorensen, J. B.; Kirschner, K. N. Calculating interaction energies using first principle theories: Consideration of basis set superposition error and fragment relaxation. *J. Chem. Educ.* **2007**, *84*, 1225−1229.
(29) DeLano, W. L.; Schrödinger, L. L. C., PyMOL(TM) Molecular Graphics System, Version 2.6.0a0. **2021**.
(30) Largent, R. J.; Polik, W. F.; Schmidt, J. R. Symmetrizer: Algorithmic determination of point groups in nearly symmetric molecules. *J. Comput. Chem.* **2012**, *33*, 1637−1642.
(31) Hunter, J. D. Matplotlib: A 2D graphics environment. *Computing In Science & Engineering* **2007**, *9*, 90−95.
(32) Harris, C. R.; Millman, K. J.; van der Walt, S. J.; Gommers, R.; Virtanen, P.; Cournapeau, D.; Wieser, E.; Taylor, J.; Berg, S.; Smith, N. J.; et al. Array programming with NumPy. *Nature* **2020**, *585*, 357−362.
(33) W.., McKinney, Data Structures for Statistical Computing in Python. *Proceedings of the 9th Python in Science Conference*. **2010**; pp 56-61, .
(34) The Pandas Development Team, pandas-dev/pandas: Pandas. https://pandas.pydata.org (last accessed July 23, 2025), 2020.
(35) Sinha, P.; Boesch, S. E.; Gu, C.; Wheeler, R. A.; Wilson, A. K. Harmonic Vibrational Frequencies: Scaling Factors for HF, B3LYP, and MP2Methods in Combination with Correlation Consistent Basis Sets. *J. Phys. Chem. A* **2004**, *108*, 9213−9217.
(36) Jensen, H. B.; Brodersen, S. The totally symmetric rotation-vibrational Raman bands of benzene. *J. Raman Spectrosc.* **1979**, *8*, 103−110.
(37) Plíva, J.; Pine, A. S. The spectrum of benzene in the 3-μm region: The ν_{12} fundamental band. *J. Mol. Spectrosc.* **1982**, *93*, 209−236.
(38) Plíva, J.; Johns, J. W. C. The ν_{13} fundamental band of benzene. *Can. J. Phys.* **1983**, *61*, 269−277.
(39) Plíva, J.; Johns, J. W. C. The perpendicular band ν_{14} of benzene near 10 μm. *J. Mol. Spectrosc.* **1984**, *107*, 318−323.
(40) Esherick, P.; Owyoung, A.; Plíva, J. Ionization-detected Raman studies of the 1600 cm^{-1} Fermi dyad of benzene. *J. Chem. Phys.* **1985**, *83*, 3311−3317.
(41) Berman, J. M.; Goodman, L. The a_{2g} mode in ground state benzene. *J. Chem. Phys.* **1987**, *87*, 1479−1487.

https://doi.org/10.1021/acs.jpca.5c03923
J. Phys. Chem. A 2025, 129, 8110−8119

(42) Pliva, J.; Johns, J. W. C.; Lu, Z. High-Resolution Study of the Difference Band ν_{17} - ν_{20} of Benzene. *J. Mol. Spectrosc.* **1993**, *161*, 269−274.
(43) Plíva, J.; Johns, J. W. C.; Lu, Z. The difference bands ν_{11}-ν_4 and ν_{10}-ν_{18} of benzene at high resolution. *Mol. Phys.* **1996**, *87*, 859−863.
(44) Cané, E.; Miani, A.; Trombetti, A. The ν_6, ν_7, ν_8 and ν_{19} gas phase fundamental frequencies of $^{12}C_6H_6$. *Chem. Phys. Lett.* **1997**, *272*, 83−85.
(45) Martin, J. M. L.; Taylor, P. R.; Lee, T. J. The harmonic frequencies of benzene. A case for atomic natural orbital basis sets. *Chem. Phys. Lett.* **1997**, *275*, 414−422.
(46) Käser, S.; Boittier, E. D.; Upadhyay, M.; Meuwly, M. Transfer Learning to CCSD(T): Accurate Anharmonic Frequencies from Machine Learning Models. *J. Chem. Theory Comput.* **2021**, *17*, 3687−3699.
(47) Jorgensen, W. L.; Severance, D. L. Aromatic-aromatic interactions: free energy profiles for the benzene dimer in water, chloroform, and liquid benzene. *J. Am. Chem. Soc.* **1990**, *112*, 4768−4774.
(48) Garrett, A. W.; Severance, D. L.; Zwier, T. S. Multiphoton ionization studies of C_6H_6-$(CH_3OH)_n$ clusters. I. Comparisons with C_6H_6-$(H_2O)_n$ clusters. *J. Chem. Phys.* **1992**, *96*, 7245−7258.
(49) Cybulski, S. M.; Lytle, M. L. The origin of deficiency of the supermolecule second-order Møller-Plesset approach for evaluating interaction energies. *J. Chem. Phys.* **2007**, *127*, 141102.
(50) Pitoňák, M.; Neogrády, P.; Černý, J.; Grimme, S.; Hobza, P. Scaled MP3 Non-Covalent Interaction Energies Agree Closely with Accurate CCSD(T) Benchmark Data. *ChemPhysChem* **2009**, *10*, 282−289.
(51) Healy, E. F.; Holder, A. An evaluation of AM1 calculated vibrational frequencies. *Journal of Molecular Structure: THEOCHEM* **1993**, *281*, 141−156.
(52) Moran, D.; Simmonett, A. C.; Leach, F. E.; Allen, W. D.; Schleyer, P. v. R.; Schaefer, H. F. Popular Theoretical Methods Predict Benzene and Arenes To Be Nonplanar. *J. Am. Chem. Soc.* **2006**, *128*, 9342−9343.
(53) Samala, N. R.; Jordan, K. D. Comment on a spurious prediction of a non-planar geometry for benzene at the MP2 level of theory. *Chem. Phys. Lett.* **2017**, *669*, 230−232.

https://doi.org/10.1021/acs.jpca.5c03923
J. Phys. Chem. A 2025, 129, 8110−8119